Nanoembossment of Au Patterns on Microspheres

Gang Zhang, Dayang Wang,* and Helmuth Möhwald

Max Planck Institute of Colloids and Interfaces, D-14424, Potsdam, Germany

Received February 13, 2006. Revised Manuscript Received June 23, 2006

This article successfully demonstrates a facile and efficient way to nanoemboss a diversity of Au patterns on microspheres by combining templating with colloidal crystals, plasma etching, and gold vapor deposition. The dimension and geometry of the Au patterns constructed on the spheres are strongly dependent on the crystal structures, the plasma etching period, and the incidence angle of Au vapor flow, yet independent of the curvature and surface chemistry of the spheres. The potential of using the resulting Au patterns on microspheres as masks for plasma etching the spheres themselves was also successfully demonstrated.

Introduction

Thanks to enormous efforts of colloidal chemists in the past decades, numerous organic and inorganic materials can now be sculptured into monodisperse micrometer-size colloidal particles predominantly with spherical shape.[1] Despite well-established surface modification techniques of colloidal particles, the functionality of their whole surface has been symmetrically identical so far, which enables particle to self-assembly only into simple hexagonal or square packing arrays, so-called colloidal crystals.[2] The achievement of higher structural complexity of colloidal crystals, for instance, the diamond structure, necessitates creation of discrete functional sites on the surfaces of colloidal particles to precisely program the interaction between the particles. Most recently, colloidal particles with patterned surface chemistry and bizarre self-assemblies have drawn emerging theoretical interest.[3] Up to now, however, there has been limited experimental work on generating patterns on colloidal particles.

Fitzmaurice and co-workers recently succeeded in selectively immobilizing one gold nanoparticle or their aggregates on one silica sphere by using nanoporous membranes as masks for infiltrating the nanoparticles.[4] This method requires a deliberate selection of the membrane pore size, the nanoparticle size, and the silica sphere diameter. It also enables decoration of only one domain on the spheres. While the use of controlled gold vapor deposition allows construction of half a gold shell on colloidal spheres, this simple strategy is not able to form complicated patterns on the spheres.[5]

Nowadays the creation of sophisticated patterns relies mainly on state-of-the-art lithography.[6] Patterns with minimal feature dimensions of less than 100 nm become routinely accessible. Nevertheless, the current lithographic strategies allow fabrication of patterns only on planar surfaces; they are exceedingly difficult to be applied on nonplanar surfaces due to a lack of appropriate masks. On the basis of the integration of self-assembly and lithography, Whitesides and co-workers have developed a so-called soft lithography.[7] This technique may provide a capability to pattern curved surfaces.[8] However, it is not yet able to pattern nonplanar surfaces with curvatures of less than 25 μm.

Van Duyne and others have employed ordered arrays of interstices within single or double-layered colloidal crystals as masks for chemical vapor deposition to construct patterns on two-dimensional planar substrates, paving a new way of lithography, so-called nanosphere lithography.[9] The dimension and shape of the resulting patterns may be easily manipulated by the sizes of the spheres and their packing structures. Most recently we have successfully demonstrated the potential to extend this nanosphere lithography to pattern microsphere surfaces.[10] By using the ordered interstices on the top single or double layers of colloidal crystals as masks for gold vapor deposition, we found that various gold patterns have been constructed on the spheres in the lower layers, showing a dependence on the crystal structures of the templates.[10] Herein we present the detailed exploration of embossment of gold patterns on microspheres by utilizing colloidal crystals as templates during gold vapor deposition. Yang and co-workers recently succeeded in employing

* Corresponding author. Fax: 49-331-5679202. E-mail: dayang.wang@mpikg-golm.mpg.de.

(1) For reviews, see: (a) Blackley, D. C. *Polymer Latices: Science and Technology*, 2nd ed.; Chapman and Hall, London, 1997; Vol. 2. (b) Matijevic, E. *Chem. Mater.* **1993**, *5*, 412.
(2) For reviews, see: a) Wang, D.; Möhwald, H. *J. Mater. Chem.* **2004**, *14*, 459. (b) Xia, Y.; Gates, B.; Yin, Y.; Lu, Y. *Adv. Mater.* **2000**, *12*, 693.
(3) (a) Nelson D. R. *Nano Lett.* **2002**, *2*, 1125. (b) Zhang, Z.; Keys, A. S.; Chen, T.; Glotzer, S. C. *Langmuir* **2005**, *21*, 11547.
(4) Nagle, L.; Fitzmaurice, D. *Adv. Mater.* **2003**, *15*, 933.
(5) (a) Lu, Y.; Xiong, H.; Jiang, X.; Xia, Y.; Prentiss, M.; Whitesides, G. M. *J. Am. Chem. Soc.* **2003**, *125*, 12724. (b) Bao, Z.; Chen, L.; Weldon, M.; Chandross, E.; Cherniavskaya, O.; Dai, Y.; Tok, J. *Chem. Mater.* **2002**, *14*, 24.
(6) Arden, W. M. *Curr. Opin. Solid State Mater. Sci.* 2002, **6**, 371.
(7) Xia, Y.; Whitesides, G. M. *Angew. Chem., Int. Ed. Engl.* **1998**, *37*, 550.
(8) Jackman, R. J.; Wilbur, J. L.; Whitesides, G. M. *Science* **1995**, *269*, 664.
(9) (a) Haynes, C. L.; Van Duyne, R. P. *J. Phys. Chem. B* **2001**, *105*, 5599. (b) Haynes, C. L.; McFarland, A. D.; Smith, M. T.; Hulteen, J. C.; Van Duyne, R. P. *J. Phys. Chem. B* **2002**, *106*, 1898. (c) Kosiorek, A.; Kandulski, W.; Glaczynska, H.; Giersig, M. *Small* **2005**, *1*, 439.
(10) (a) Zhang, G.; Wang, D.; Möhwald, H. *Nano Lett.* **2005**, *5*, 143. (b) Zhang, G.; Wang, D.; Möhwald, H. *Angew. Chem., Int. Ed. Engl.* **2005**, *44*, 7767.

10.1021/cm060358f CCC: $33.50
Published on Web 07/26/2006

reactive ion beam to etch colloidal crystals in an anisotropic fashion.[11] In the current work, we reduced the size of the uppers spheres in the colloidal crystal templates with the aid of O_2-plasma etching, increasing interstices in a defined way and thus obtaining a wealth of Au patterns on microspheres. The angle-resolved Au vapor deposition was also conducted to increase the structural complexity of Au patterns on microspheres. Finally we also demonstrated the potential of using the deposited Au patterns as mask for plasma etching of microspheres to generate the nonspherical colloidal particles.

Experimental Section

Preparation of Colloidal Crystals. Samples of 10 wt % aqueous suspensions of polystyrene (PS) spheres ranging in size from 270 to 925 nm and silica spheres ranging in diameter from 300 to 520 nm were purchased from Microparticles GmbH, Germany. The crystallization of these spheres was implemented on silicon wafers or glass slides by means of dip coating. The used substrates were cleaned with piranha solution (H_2SO_4:H_2O_2 = 3:1) prior to dip coating. The thickness of the colloidal crystals obtained was controlled by the sphere concentrations and the withdrawing speeds. The sphere concentrations ranged from 1.0 to 3.0 wt %. The withdrawing speeds were optimized in the range of 0.5−5 μm/s.

On the basis of the method reported in the literature,[12] V-shaped grooves were constructed on silicon wafers by etching at 70 °C for 10 min using a mixture of water (40 mL), KOH (9.2 g) and 2-propanol (13.2 mL). On the resulting etched silicon wafers, fcc colloidal crystals with a preferential plane of (100) parallel to the substrates were constructed via dip coating.

The PS colloidal crystals obtained were etched by O_2-plasma by using a plasma cleaner (Harrick, PDC-32G, Germany) at a pressure of 0.2 mbar and a power density of 100 W. The etching period ranged from 3 to 20 min.

Gold Vapor Deposition. Gold vapor deposition on the colloidal crystals and on those etched by O_2-plasma was performed in a high vacuum coater (Edwards Auto 306, U.K.) at a pressure of 10^{-7} mbar. The deposition speed of gold was 0.02 nm/s. By varying the deposition time, 25, 40, 85, and 170 min, gold layers of 30, 50, 100, and 200 nm in thickness were deposited on the colloidal crystals, respectively. Prior to Au vapor deposition, a 5 nm thick chromium layer was deposited in the crystals in order to improve the wettability of gold on the colloidal crystals. The incidence angles between the Au vapor flow and the normal direction of the samples were adjusted to 0°, 15°, 30°, and 45° by tilting the samples on the sample holding blocks in the vapor deposition chamber. It is worthwhile to note that no distortion of colloidal spheres or the crystal structure was observed during Au vapor deposition.

Stepwise Removal of Colloidal Spheres. After gold vapor deposition, we placed double-sided adhesive tapes on the surfaces of the gold-coated colloidal crystals and subsequently placed glass slides atop the tapes. After pressing the glass slides by 0.2 kg/cm^2 for 5 min, the spheres in the top layers were stripped off, leaving behind Au patterns on the spheres in the second layers. As suggested in the literature,[13] the exclusive peeling of the top layer spheres is due to the fact that the interaction between the adhesive tape and the top layer spheres in colloidal crystals is much larger than that between the spheres in the different layers. Following the similar procedure, we peeled off the spheres layer-by-layer from the crystals for the observation of the Au patterns formed on the spheres in the underlying layers.

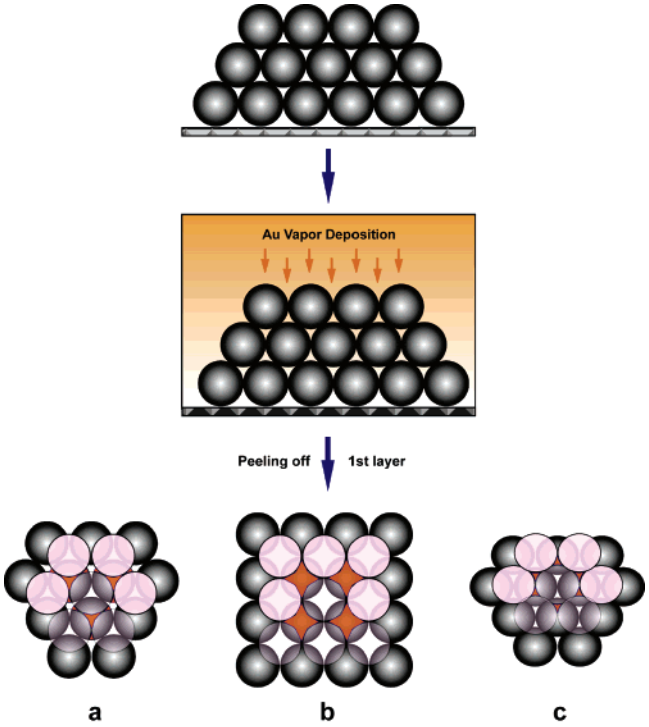

Figure 1. Schematic illustration of the procedure to emboss nanosized Au patterns on microspheres by using colloidal crystals with various preferential orientations (111) (a), (100) (b), and (110) (c), parallel to the substrates, as masks for the gold vapor deposition. The top layer is highlighted in pink. The orange areas represent the Au domains embossed on spheres after peeling off the upper layers.

Characterization. Scanning electron microscope (SEM) images were recorded by means of a Gemini LEO 1550 instrument operated at 3 kV. To directly reveal the Au patterns on colloidal spheres, in our work, the samples without Au sputter-coating were used for SEM measurements. Atomic force microscope (AFM) imaging was performed by using the Nanoscope Dimension 3100 system operating in tapping mode.

Results and Discussion

Colloidal Crystals as Templates for Gold Nanoembossement on Microspheres. Our procedure of embossing different Au patterns on microsphres is schematically illustrated in Figure 1. First, colloidal crystals with defined layer numbers were constructed on planar substrates. Second, gold thin films are deposited on the colloidal crystals. During Au vapor deposition, obviously, the gold flow can reach the spheres in the second layers in the crystals only through interstices between the top layer spheres. Accordingly, the ordered interstitial structures in the top layers may be regarded as masks to pattern the gold vapor flow, thus directing the gold deposition on the spheres in the second layer. Third, the microspheres coated with various Au patterns are obtained after peeling off the top layers. Apparently, the features of Au patterns embossed on the spheres are dependent on the packing structures of the top layers, that is, the preferential orientation of the colloidal crystals parallel to the substrates.

(11) (a) Choi, D.; Yu, H.; Jang, S.; Yang S.-M. *J. Am. Chem. Soc.* **2004**, *126*, 7019. (b) Choi, D.; Jang, S.; Kim, S.; Lee, E.; Han, C.; Yang S.-M. *Adv. Funct. Mater.* **2006**, *16*, 33.
(12) (a) Yang, S.; Ozin G. *Chem. Commun.* **2000**, 2507. (b) Yin, Y.; Xia, Y. *Adv. Mater.* **2002**, *14*, 605.
(13) Yao, J.; Yan, X.; Lu G.; Zhang, K.; Chen, X.; Jiang, L.; Yang, B. *Adv. Mater.* **2004**, *16*, 81.

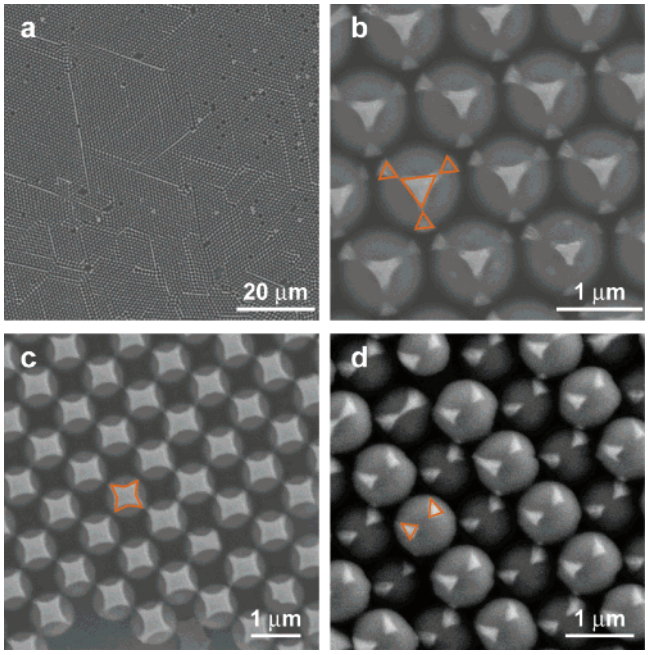

Figure 2. Low (a) and high (b) magnification SEM picture of 925 nm PS spheres coated with Au-patterned surfaces, generated by templating the top monolayers of colloidal crystals with (111) facets parallel to the substrates during Au vapor deposition. Bright spots correspond to Au domains on spheres. SEM pictures of 925 nm polystyrene spheres with Au-patterned surfaces generated by using the top monolayers of colloidal crystals with preferential crystal orientation of (100) (c) and (110) (d) parallel to substrates, as masks. The gold layers deposited on the crystals are 30 nm in thickness.

When the preferential orientation of colloidal crystals is (100) parallel to the substrates, the square interstices within the top layer are exclusively blocked by the spheres in the underlying layer (Figure 1b). Using this crystal facet as a template, we constructed the square Au domains on the top of the spheres (Figure 2c). When the preferential orientation of colloidal crystals is (110) parallel to the substrates, two triangular interstices within the top layer are exclusively blocked by one sphere in the underlying layer (Figure 1c). By using (110) crystal facets as masks, two triangular Au dots were obtained on the spheres in the second layers, as shown in Figure 2d.

It is noteworthy that the present approach enables embossment of the Au patterns, shown in Figure 2, on PS spheres of different diameters, ranging from 925 to 270 nm (Figure S1). Approximately 10^8-10^9 microspheres on 1 cm^2 silicon wafers can be patterned by using the present approach. Besides on PS spheres, we also succeeded in constructing these Au patterns on differently sized silica spheres (Figure S2). These indicate that our approach is independent of the dimension and the surface chemical nature of the microspheres used. Nevertheless, it is fairly difficult to precisely determine the highly curved cross-section profiles of nanosized Au domains embossed on the microspheres, even with the aid of AFM and tilted-angle SEM.

Van Duyne and co-workers have demonstrated that not only the ordered interstitial array within the close packed sphere monolayer but also the array within the close packed sphere bilayers can be used as masks to generate Au patterns on planar surfaces.[9] Nonetheless, when the top bilayers of colloidal crystals are used as templates to emboss Au patterns

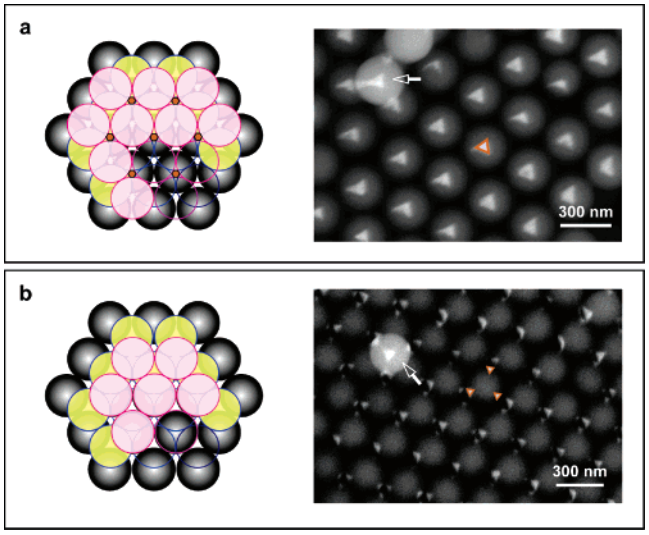

Figure 3. SEM pictures of PS microspheres coated with Au patterns, obtained by templating the upper double layers of (111) facets of their colloidal crystals with an ABCABC (a) and ABAB (b) stacking symmetry. The corresponding schematic illustrations are shown in the left, in which the top first and second layer spheres are highlighted in pink and yellow, respectively. The PS spheres are 270 nm in diameter and the gold layers deposition on the crystals are 30 nm in thickness.

on the third layer spheres, one has to take into account both the crystal orientation and the stacking symmetry of the spheres. When the (100) or (110) facets of colloidal crystals are parallel to the substrates, the interstices within the top layers are completely blocked by the spheres in the second layers, so the Au flow cannot reach the spheres in the third layers (Figure S3). When the preferential orientation of colloidal crystals is (111) parallel to the substrates, as suggested in the literature, [9] the Au flow may still reach the spheres in the third layers. In this scenario, the stacking symmetry of the spheres appears to influence the Au patterns embossed on the third layer spheres. When the stacking symmetry of the spheres in colloidal crystals is ABCABC, the spheres in the second layer may block only half of the interstices in the top layer, while the interstices between them are located beneath another half of the interstices in the top layer, leading to a small void atop each third layer sphere for the penetration of Au vapor flow (left in Figure 3a). By templating ABCABC stacked (111) facets of colloidal crystals, accordingly, we obtained one Au dot in each sphere in the third layer (Figure 3a). These Au dots atop the third layer spheres are rather small as compared to those embossed on the second layer spheres (Figure S1b).

In colloidal crystals, there de facto coexist both ABCABC and ABAB stacking symmetry due to the exceedingly narrow energy difference between them. When the stacking symmetry of the spheres within colloidal crystals is ABAB, underneath half of the interstices within the upper layers are positioned exclusively the interstices between the spheres in the underlying layers, thus leaving behind the air channels that allow Au vapor to freely penetrate through the whole colloidal crystal and to reach the substrate (left in Figure 3b). During the penetration, Au vapor may condense at the edge of the lower spheres in the colloidal crystals. As shown in Figure 3b, each sphere in the third layers was decorated with three small Au dots by using ABAB stacked (111) facets to template Au vapor deposition. These three Au dots on

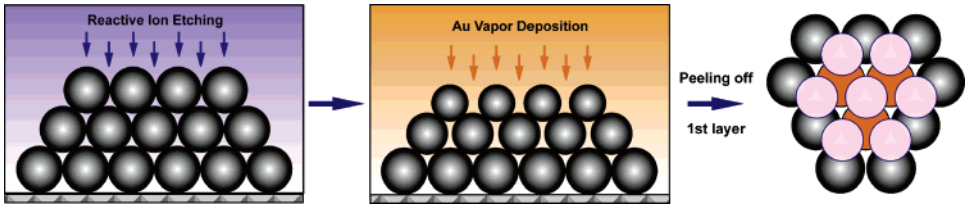

Figure 4. Schematic illustration of nanoembossment of Au patterns on microspheres by using O_2-plasma etched colloidal crystals as masks for Au vapor deposition. The top layer is highlighted in pink. The orange areas represent the Au domains embossed on spheres after peeling off the upper layers.

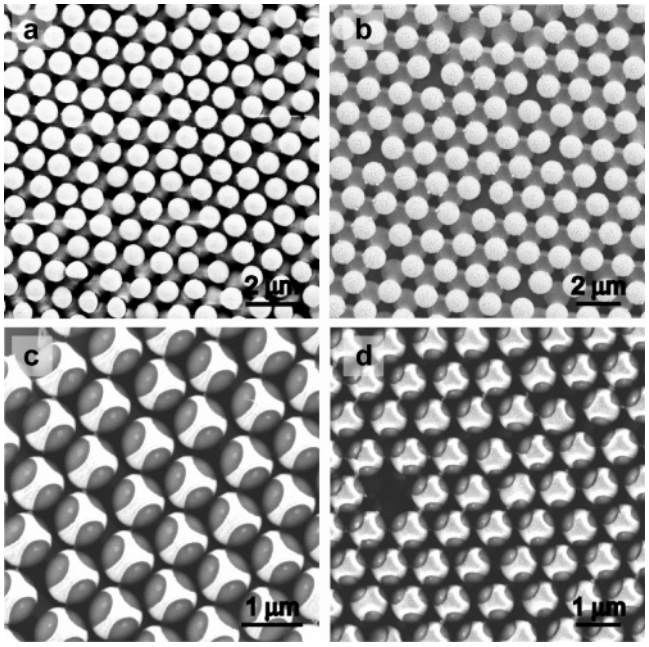

Figure 5. SEM images of gold-coated 925 nm PS colloidal crystals, etched by O_2-plasma for 10 (a) and 20 min (b). The preferential orientation of the crystals is (111) parallel to the substrates. The gold layers are 100 nm in thickness. The corresponding SEM images of the Au patterns formed in the second spheres, after peeling off the top monolayers in these crystals, are shown in panels c and d.

the edges of the third layer spheres are smaller than those formed on the edge of the second layers (Figure S1b), likely due to the smaller interstices within the upper double layers. As the interstices within colloidal crystals dramatically decrease with the layer numbers, we hardly observed the embossment of Au on the forth or lower layers.

Plasma-Etched Colloidal Crystals as Templates for Gold Nanoembossement on Microspheres. To widen the interstices within colloidal crystals, we etched PS colloidal crystals with O_2-plasma. Figure 4 schematically represents the gold embossment on PS microspheres by using their colloidal crystals as masks during Au vapor deposition with the assistance of O_2-plasma etching.

Figure 5a,b and Figure S4 reveal SEM images of O_2-plasma-etched 925 nm PS colloidal crystals with (111) facets parallel to the substrates, showing the noticeable decline of the PS sphere diameters with the O_2-plasma etching period. The diameters of the top layer spheres, directly exposed to the O_2-plasma flow, dramatically reduced from 925 to 750 and 580 nm after 10 and 20 min etching (Figure 5a,b).

It is worthwhile to note that the center-to-center distances between the spheres remain little changed, about 925 nm, indicating that the O_2-plasma etching does not deteriorate the ordered packing structure of the colloidal crystals, as shown in Figures 5 and S4. Thus, the plasma etching efficiently enlarged the voids between the top layer spheres. By employing 10 min etched top single layers as masks, T-shaped Au domains were constructed on the second layer spheres (Figure 5c). On the other hand 20 min etched top single layers templated the formation of larger Au domains with a distorted triangular shape on the second layers (Figure 5d). In the case of using (100) facets of colloidal crystals as templates, the longer plasma etching led to almost half a gold shell (Figure S5).

During the O_2-plasma etching, as suggested in the literature,[11] the upper layers in colloidal crystals may be considered as masks for etching the underlying layers, so the etching is anisotropic, and the edges of the underlying layer spheres are etched more than their central parts just beneath the top layer spheres. This leads to a prominent enlargement of the interstitial spaces within colloidal crystals, which favors the Au vapor to penetrate into the lower layers in the crystals.

When the (111) facets of the plasma etched colloidal crystals were utilized as templates for Au vapor deposition, larger triangular Au dots were formed in the third layer spheres as compared to those derived from the nonetched crystals;[9b] one dot on each layer sphere derived from the ABCABC stacking symmetry (Figure 6a) and three dots from the ABAB stacking symmetry (Figure 6b). More intriguingly, the depth-dependent plasma etching—the upper layers were etched more than the lower layers—created open interstitial spaces in the upper double layers in (100) facets of colloidal crystals,[9b] which allow Au vapor to reach the third layers (Figure 6c). Accordingly, we obtained four Au domains on each sphere in the third layers by using (100) facets of their plasma etched colloidal crystals as masks (left in Figure 6c). This feature is not observed by templating with nonetched colloidal crystals (Figure S3).

Figure 7 reveals that after etching by O_2-plasma, the enlarged interstitial spaces in colloidal crystals allowed Au vapor to reach not only the spheres in the third layers but those in the forth layer also, especially for colloidal crystals with an ABAB stacking symmetry. Compared with that formed on the third layer spheres, the Au dots on the forth layers are fairly small. In our work, Au patterns were hardly observed on the fifth layers or lower. This may be due to the fact that because of low-power O_2-plasma usedin our work, the interstitial spaces between the upper layer spheres were not sufficiently large to allow Au vapor to reach the spheres underneath the forth layer.

Since the Au domains obtained on the spheres by templating with plasma-etched colloidal crystals are larger and their surfaces smoother than those generated from nonetched

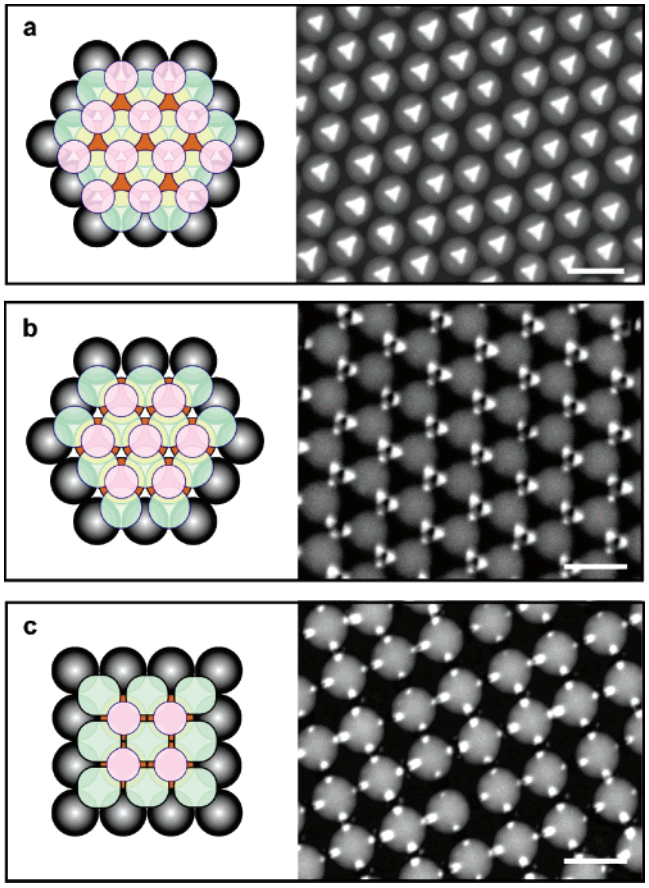

Figure 6. SEM images of 270 nm PS spheres with Au-patterned surfaces, obtained by using (111) facets of their colloidal crystals, etched by O_2-plasma for 3 min, with an ABCABC (a) and ABAB (b) stacking symmetry, by using (100) facets of their colloidal crystals (c). The gold layers are 100 nm in thickness. The corresponding schematic illustrations of the resulting coated spheres are shown on the left, in which the top first and second layer spheres are highlighted in pink and yellow, respectively. The scale bars are 300 nm.

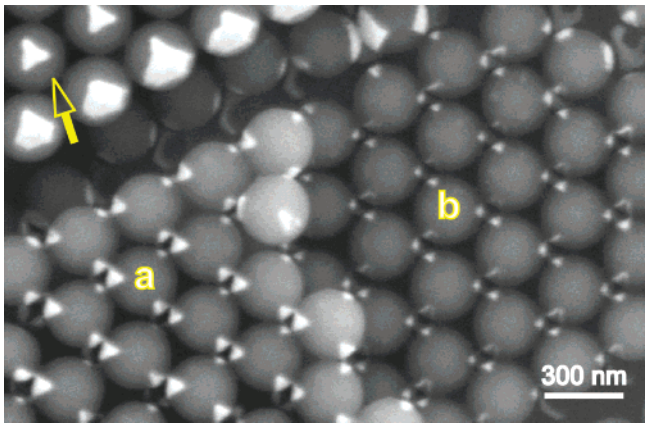

Figure 7. SEM image of Au patterns obtained on the third (a) and fourth (b) layer spheres by templating 270 nm PS colloidal crystals, etched by O_2-plasma for 3 min, with (111) facets parallel to the substrates and an ABAB stacking symmetry. The gold layers are 100 nm in thickness. The arrow indicates the Au patterns on the third layer spheres derived from ABCABC stacked (111) facets.

colloidal crystals, we were able to analyze their cross-section profiles by means of AFM (Figure S6). Figure 8 shows that the maximal height of the Au domains increases with the Au mass deposited in a rather linear way. In addition, the Au domains on the second layer spheres are noticeably thicker than those on the third layer spheres (Figure 8), consistent with their size dependence on the layer numbers derived from their SEM images.

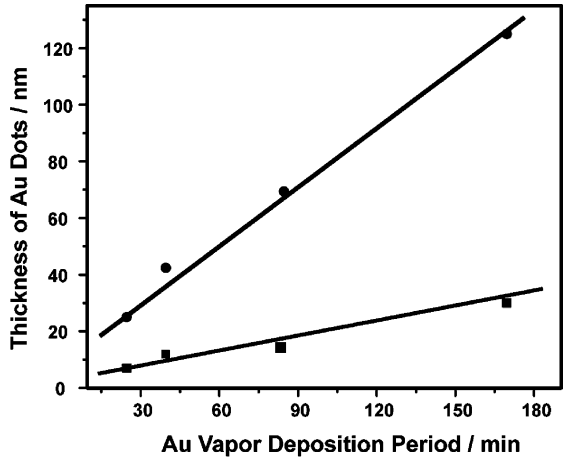

Figure 8. Plot of maximal heights of Au domains embossed on the second (solid circle) and third (solid square) layer spheres vs the Au vapor deposition period. The corresponding SEM images of these Au patterns are shown in Figure 5c and Figure 6a.

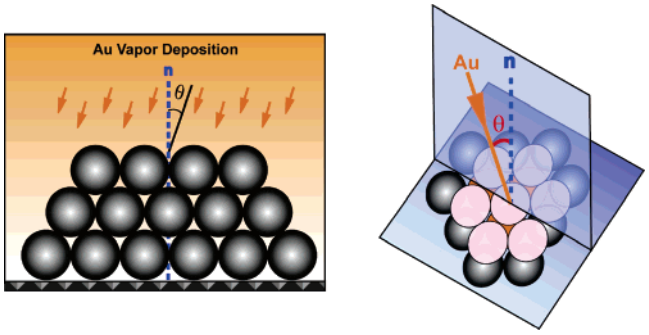

Figure 9. Schematic depictions of angle-resolved nanoembossment of Au patterns on microspheres by using their crystals as masks during Au vapor deposition. The incident angle of Au vapor flow, θ, is defined as the angle between the incident direction of Au vapor flow and the normal direction of the samples.

Angle-Resolved Gold Nanoembossment on Microspheres. In our nanoembossment procedure, reminiscent of nanosphere lithography,[9] it is evident that the projections of the interstices in the upper layers onto the underlying spheres determine the geometry and size of the Au patterns deposited on the underlying spheres. The incidence angle of the Au vapor flow has been demonstrated as an efficient measure to manipulate the projection features of the interstices.[9] In the present work, we accordingly conducted angle-resolved Au vapor deposition on colloidal crystals to achieve a higher structural complexity of the Au patterns embossed on microspheres, schematically shown in Figure 9.

When the incidence angle, θ, between the normal direction of the samples and the Au vapor flow was 15° during the Au vapor deposition, followed by peeling off the top layers, we obtained one big and one small Au triangular dot on each sphere in the second layers by templating with the (111) facets of colloidal crystals (Figure 10a). The resulting Au patterns are distinct from those derived from the incidence angle of zero shown in Figure 2b; the sizes of the Au dots obtained are smaller. The incidence angle of 30° yielded two much smaller triangular Au dots on the second layer spheres (Figure 10b). When we conducted Au vapor deposition on

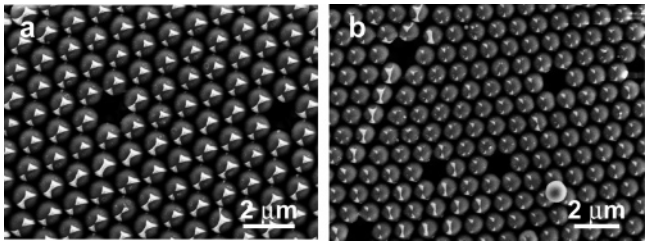

Figure 10. SEM images of 925 nm PS spheres with Au-patterned surfaces, obtained by using the top monolayers of (111) facets of their colloidal crystals as masks during Au vapor deposition at varied incident angles, θ of 15° (a) and 30° (b). The gold layers deposited on the crystals are 100 nm in thickness.

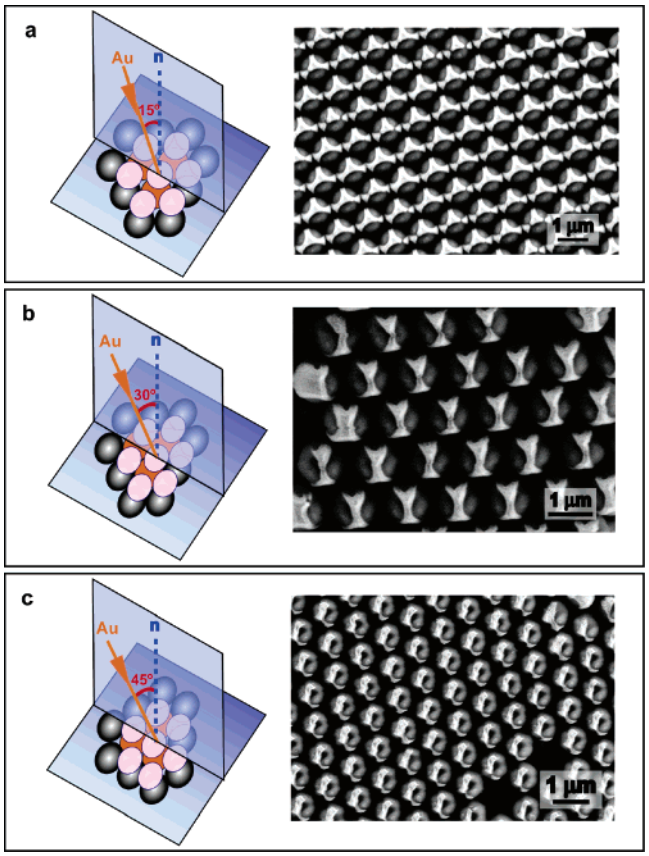

Figure 11. SEM images of 925 nm PS spheres with Au-patterned surfaces, obtained by using the top monolayers of (111) facets of 10 min plasma etched colloidal crystals as masks during Au vapor deposition at varied incident angles, θ of 15° (a), 30° (b), and 45° (c). The corresponding schematic illustrations of the resulting Au patterns are shown on the left. The gold layers deposited on the crystals are 100 nm in thickness.

colloidal crystals at θ larger than 30°, however, few Au patterns were found on the second layer spheres, suggesting that the interstices between the top layer spheres were little projected onto the second layer spheres.

Since the O_2-plasma etching may sufficiently increase the interstitial spaces in colloidal crystals, we also conducted angle-resolved Au nanoembossment of microspheres by using plasma-etched crystals as masks for Au vapor deposition. When (111) facets of O_2-plasma-etched PS colloidal crystals were used as masks and Au vapor deposition was implemented at θ of 15°, as shown in Figure 11 a, the Au patterns obtained on the second layer spheres exhibited a transition feature between those shown in Figures 2b and 5c.

When the Au vapor deposition was performed at θ of 30°, I-shaped Au dots were obtained on the second layer spheres

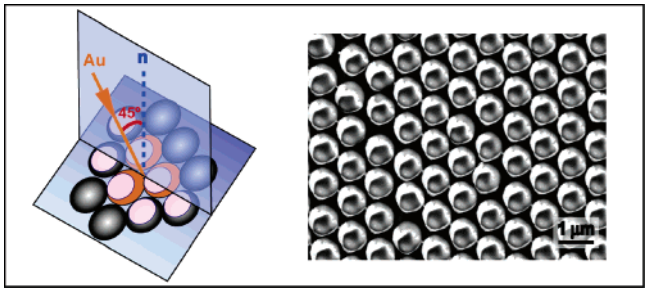

Figure 12. SEM image of 925 nm PS spheres with Au-patterned surfaces, obtained by using the top monolayers of (111) facets of 20 min plasma etched colloidal crystals as masks during Au vapor deposition at the incident angles, θ of 45°. The corresponding schematic illustration of the resulting Au patterns is shown on the left. The gold layers deposited on the crystals are 100 nm in thickness.

(Figure 11b). Figure 11c shows that the deposition of Au vapor at θ of 45° led to the L-shaped Au domains atop the second layer spheres, indicating that the interstices between the top layer spheres, enlarged by plasma etching, are capable of projection on the second layer spheres. When the interstitial sizes between the top layer spheres were further increased by prolonging the plasma etching period to 20 min, interestingly, the second spheres were capped by ring-shaped Au domains, and no Au dots were deposited on them (Figure 12). These resulting new patterns are not obtained otherwise. Due to the large dimension of the interstices within colloidal crystals with a preferential orientation of (100), square Au patterns derived from them show a smaller variation during angle-resolved Au vapor deposition (Figure S7).

The incident angle of Au vapor flow allowed us not only to create unusual Au patterns on the second layer spheres but also to alter the patterns on the third layer spheres. The slightly larger incident angle, θ of 10° for instance, led to reduction of the Au dot numbers embossed on each third layer sphere, from three to two dots by templating with the ABAB stacked (111) facets of colloidal crystals (Figure S8a) and from four to three dots by using the crystals with (100) facets parallel to the substrates (Figure S8b).[9b] However, after further increase of the incident angle, no Au patterns were observed on the third layer spheres due to the fairly small interstices in the upper double layers.

Modeling of Au Patterns Embossed on Microspheres. To figure out the influence of experimental variables—such as the template sphere size, the incident angle of the Au flow, and the plasma etching degree—on the Au patterns embossed on microspheres, we present a simple modeling based on the geometry of colloidal crystals. Figure 13 illustrates the geometric feature of the closely packed microspheres in the top layer of colloidal crystals. When no diffraction of the Au flow was assumed, the Au flow can reach to the spheres in the second layer of a colloidal crystal only through the interstices in the top layer. As a result, the feature of Au patterns deposited on the second layer spheres is determined by the feature of the projection area of the Au flow on the interstitial spaces of the top layers, highlighted by yellow in Figure 13. The angle bisector length of the triangle projection, *a* underlined by the orange line in Figure 13, was used to represent the size of the large triangle Au domain obtained on the second layer spheres (shown in Figure 2b).

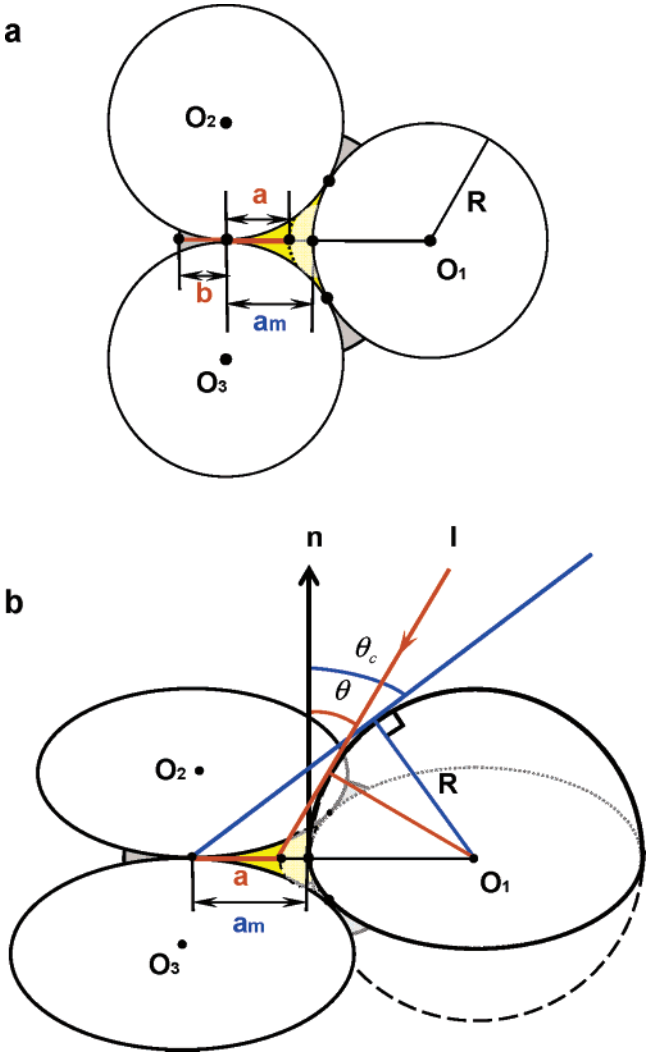

Figure 13. Schematic illustration of the geometric features of the close-packed microspheres in a colloidal crystal. (a) is a top-view of the closely packed three spheres and (b) their quasi-3D illustration. O_1, O_2, and O_3 are the centers of the three spheres, and R is their radius. a and b are the heights of two projection area of the Au flow on the interstitial spheres in the top layers, underlined by orange lines, and a_m represents the maximum value. n points the normal direction of the equator plane of the three spheres. The orange line represents the incidence of the Au flow, and the maximal incidence angle, θ_c, is underlined by the blue line.

On the basis of simple geometry analysis (details in Supporting Information), a can be easily calculated by

$$a = \sqrt{3}R - \frac{R}{\cos\theta} = R\left(\sqrt{3} - \frac{1}{\cos\theta}\right) \qquad (1)$$

in which R is the radius of the microspheres and θ the incident angle of the Au flow. When θ is zero, a reaches the maximum, $a_m = R(\sqrt{3} - 1)$, in agreement with the previous report.[9a,b] This suggests formation of the largest Au patterns on the second layer spheres. As suggested in Equation 1, the Au pattern dimension or the **a** value decreases with the increase of θ. When the θ is larger than a critical value, a turns out zero; no Au pattern is formed. This is rather consistent with the aforementioned SEM results. On the basis of Figure 13, the critical value, θ_c, is calculated as 54.74° (Supporting Information), consistent with literature.[9a,b]

On the other hand, the size of the small triangle Au domains located at the edges of the second layer spheres (shown in Figure 2b) can be estimated by the following equation (details in Supporting Information):

$$b = R\left(1 - \frac{1}{\sqrt{3}}\right) \qquad (2)$$

in which θ is 0 and b the angle bisector length of the triangle Au domains as shown in Figure 13a. As suggested by eqs 1 and 2, obviously the Au pattern dimension increases with the size of the template microspheres, in agreement with the aforementioned SEM and AFM results.

When colloidal crystals were etched by O_2 plasma, the interstices in the top layers turned out rather larger, allowing formation of the large Au patterns on the second layer spheres (Figure 5c,d). In this case, the dimension of Au patterns formed on the second layer in an etched colloidal crystal can be evaluated as follows (details in Supporting Information):

$$a_p = R\left(\frac{2}{\sqrt{3}} + \beta - \frac{\alpha}{\cos\theta}\right) \qquad (3)$$

in which a_p is the size of the triangular Au patterns, α is the shrinkage degree of the top layer spheres (R_1) as compared with the original ones ($\alpha = (R_1/R)$), and β is the shrinkage degree of the second layer spheres (R_2) ($\beta = (R_2/R)$). The comparison between eqs 1 and 3 indicates that the sizes (a_p) of the Au domains derived from etched colloidal crystals roughly equal to the sum of the sizes of the large (a) and small (b) Au domains from nonetched colloidal crystals, $a_p = a + b$ (Supporting Information), which is due to the fact that the top layer spheres become nontouched after plasma etching. This also suggests a consistency of the present modeling albeit it is rather simple and rough. When θ equals zero, the maximum value of a_p, a_{pm}, is achieved, $a_{pm} = R((2/\sqrt{3}) + \beta - \alpha)$. Nonetheless, when θ becomes larger than a critical value, $\theta_{pc} = \arccos(3\sqrt{3}\alpha/2 + 3\sqrt{3}\beta)$ (details in Supporting Information), no Au pattern is obtained on the second layer spheres.

On the basis of eqs 1−3, we calculated the sizes of Au patterns derived from the colloidal crystals used in the present work, which were summarized in Table 1. Although the present modeling was rather rough, the calculated values were rather comparable with the experimental ones measured from the SEM pictures; the latter was slightly larger than the former. This small deviation was also reported in the literature,[9a] which may suggest the small diffraction of Au beams during the deposition into colloidal crystals.

Table 1. Sizes of Au Patterns on Microspheres Derived from the Top Monolayers in Their Colloidal Crystals

au patterns	calculated data	experimental data[a]
larger domain in Figure 2b	339 nm[b]	358 ± 18 nm
small domain in Figure 2b	196 nm[c]	217 ± 12 nm
patterns in Figure 5c	615 nm[d]	672 ± 40 nm
patterns in Figure 5d	618 nm[e]	686 ± 40 nm
patterns in Figure 11a	548 nm[f]	555 ± 30 nm

[a] Measured from the corresponding SEM pictures. [b] Calculated by eq 1 and $\theta = 0$. [c] Calculated by eq 2 and $\theta = 0$. [d] Calculated by eq 3 and $\theta = 0$, $\alpha = 0.79$, and $\beta = 0.97$, measured from the corresponding SEM picture. [e] Calculated by eq 3 and $\theta = 0$, $\alpha = 0.74$, and $\beta = 0.93$, measured from the corresponding SEM picture. [f] Calculated by eq 3 and $\theta = 15°$, $\alpha = 0.89$, and $\beta = 0.96$, measured from the corresponding SEM picture.

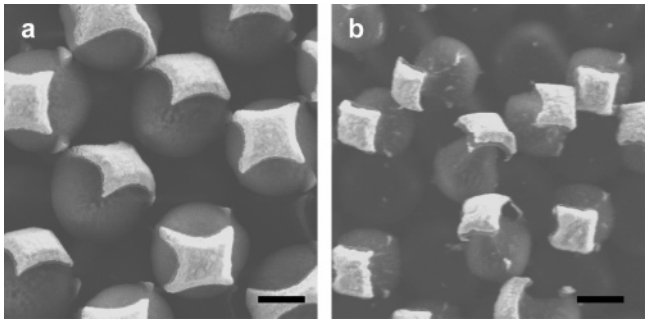

Figure 14. SEM pictures of 10 (a) and 20 min (b) O_2-plasma etched 925 nm PS spheres coated with square Au patterns, whose initial structures are shown in Figure 2c. The scale bars are 500 nm.

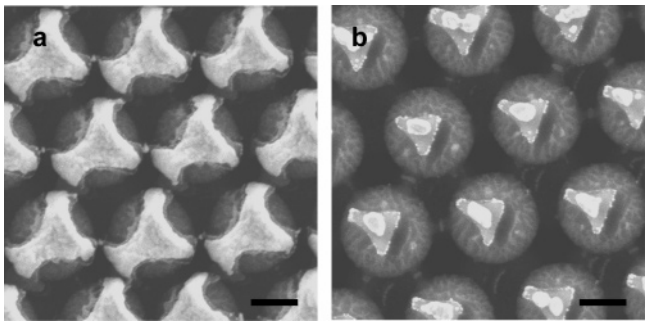

Figure 15. SEM pictures of 10 min O_2-plasma etched 925 nm PS spheres coated with triangular Au patterns obtained from templating the top single (a) or double (b) layer, whose initial structures are shown in Figures 5c and 6a. The scale bars are 500 nm.

Etching Microspheres by Using Their Au Patterns as Masks. As Au patterns embossed on microspheres should exhibit a distinct resistance against the O_2-plasma compared to the spheres themselves, in our work, they were recruited as masks to selectively etch the uncoated parts of the spheres. By using the square Au domains on the microspheres derived from (100) facets of colloidal crystals (shown in Figure 2c) as masks for O_2-plasma etching, we were able to transform the spheres into asymmetric drop-like particles with square Au caps in 10 and 20 min (Figure 14a,b). Figure 14 also clearly demonstrates the nonuniform character of the cross-section profile of the Au patterns formed on microspheres—the central part is much thicker than the edge, consistent with the AFM observation.

By using the big triangular Au domains (Figure 5c), derived from plasma-etched (111) facets of colloidal crystals, as etching masks, Figure 15a shows that without Au protection, uncoated parts of the spheres were selectively severely etched. By the triangular Au patterns on the third layer spheres as plasma etching masks for the spheres, symmetric spherical particles were etched into asymmetric drop-like particles with triangular Au caps (Figure 15b). In this case, note that as the plasma etching implemented in our work was associated with heating, the fusion of Au patterns often took place during the longer period of etching, thus forming big Au dots atop the resulting etched particles (Figure 15b). To use the Au patterns embossed on microspheres as masks for reactive ion etching of the spheres themselves, especially with intent to avoid the aforementioned heating effect, is one of the ongoing research projects in our lab.

Conclusion

Overall, we have successfully demonstrated a facile and generally applicable method of Au nanoembossment on microspheres. By using the upper layer spheres in colloidal crystals as masks for Au vapor deposition, diverse Au nanosized patterns were embossed on the lower spheres. The use of plasma etched colloidal crystals as templates and the angle-resolved Au vapor deposition allow achievement of a higher structural complexity of Au patterns. The geometry and dimension of the resulting patterns are dependent on the crystal orientations of the colloidal crystal templates used, the upper layer numbers, the incident angles of Au vapor flow, and the plasma etching period. At the meantime, our methodology presents an independence of the size and the surface chemical nature of the spheres. These effects of experimental parameters on the dimension of the Au patterns obtained, especially on the second layer spheres, were analyzed based on a simple geometry modeling. In addition, we also successfully demonstrated the potential of using the resulting Au patterns on microspheres as masks for the plasma etching of the spheres themselves, allowing creation of asymmetric particles with unusual shapes that are not prepared otherwise. Since the Au patterns embossed on microspheres may provide functional sites to direct the spatial coupling between the spheres, the resulting coated spheres should be regarded as new generation building blocks for colloidal self-assembly, enabling one to translate the supramolecular chemistry language to create hierarchical "supraparticles".[3,14]

Acknowledgment. We thank the Max Planck Society for the financial support.

Supporting Information Available: Additional SEM images, figures and text on modeling the nanoembossment of Au patterns on microspheres. This material is available free of charge via the Internet at http://pubs.acs.org.

CM060358F

(14) Manoharan, V. N.; Elsesser, M. T.; Pine D. J. *Science* **2003**, *301*, 483.